Arbitrary GRIN component fabrication in optically driven diffusive photopolymers

Adam C. Urness,[1,2,3,*] **Ken Anderson,**[3] **Chungfang Ye,**[2] **William L. Wilson**[1] **and Robert R. McLeod**[2]

[1]*Department of Materials Science and Engineering, Frederick Seitz Materials Research Laboratory, University of Illinois at Urbana-Champaign, Urbana , Il 61801 , USA*
[2]*Department of Electrical, Computer and Energy Engineering, University of Colorado Boulder, CO 80309, USA*
[3] *Akonia Holographics, Longmont, CO 80021, USA*

*urness@colorado.edu

Abstract: We introduce a maskless lithography tool and optically-initiated diffusive photopolymer that enable arbitrary two-dimensional gradient index (GRIN) polymer lens profiles. The lithography tool uses a pulse-width modulated deformable mirror device (DMD) to control the 8-bit gray-scale intensity pattern on the material. The custom polymer responds with a self-developing refractive index profile that is non-linear with optical dose. We show that this nonlinear material response can be corrected with pre-compensation of the intensity pattern to yield high fidelity, optically induced index profiles. The process is demonstrated with quadratic, millimeter aperture GRIN lenses, Zernike polynomials and GRIN Fresnel lenses.

References and links

1. D. T. Moore, "Gradient-index optics: a review," Appl. Opt. **19**, 1035–1038 (1980).
2. P. Sinai, "Correction of optical aberrations by neutron irradiation," Appl. Opt. **10**, 99–104 (1971).
3. M. A. Pickering, R. L. Taylor, and D. T. Moore, "Gradient infrared optical material prepared by a chemical vapor deposition process," Appl. Opt. **25**, 3364–3372 (1986).
4. S. Ohmi, H. Sakai, Y. Asahara, S. Nakayama, Y. Yoneda, and T. Izumitani, "Gradient-index rod lens made by a double ion-exchange process," Appl. Opt. **27**, 496–499 (1988).
5. B. Messerschmidt, T. Possner, and R. Goering, "Colorless gradient-index cylindrical lenses with high numerical apertures produced by silver-ion exchange," Appl. Opt. **34**, 7825–7830 (1995).
6. S. Ji, K. Yin, M. Mackey, A. Brister, M. Ponting, E. Baer, "Polymeric nanolayered gradient refractive index lenses: technology review and introduction of spherical gradient refractive index ball lenses," Opt. Eng. **52**, 112105–112105 (2013).
7. J.-H. Liu, P.-C. Yang, and Y.-H. Chiu, "Fabrication of high-performance, gradient-refractive-index plastic rods with surfmer-cluster-stabilized nanoparticles," J. Polym. Sci. A Polym. Chem. **44**, 5933–5942 (2006).
8. J.-H. Liu and Y.-H. Chiu, "Process equipped with a sloped uv lamp for the fabrication of gradient-refractive-index lenses," Opt. Lett. **34**, 1393–1395 (2009).
9. S. P. Wu, E. Nihei, and Y. Koike, "Large radial graded-index polymer," Appl. Opt. **35**, 28–32 (1996).
10. C. Ye and R. R. McLeod, "Grin lens and lens array fabrication with diffusion-driven photopolymer," Opt. Lett. **33**, 2575–2577 (2008).
11. B. A. Kowalski, A. C. Urness, M.-E. Baylor, M. C. Cole, W. L. Wilson, and R. R. McLeod, "Quantitative modeling of the reaction/diffusion kinetics of two-component diffusive photopolymers," Opt. Mater. Express (2014).

12. P. Wang, B. Ihas, M. Schnoes, S. Quirin, D. Beal, S. Setthachayanon, T. Trentler, M. Cole, F. Askham, D. Michaels, S. Miller, A. Hill, W. Wilson, and L. Dhar, "Photopolymer media for holographic storage at 405 nm," in "Optical Data Storage Topical Meeting 2004," (International Society for Optics and Photonics, 2004), pp. 283–288.

13. T. J. Trentler, J. E. Boyd, and V. L. Colvin, "Epoxy resin-photopolymer composites for volume holography," Chem. Mater. **12**, 1431–1438 (2000).

14. W. J. Gambogi Jr, K. W. Steijn, S. R. Mackara, T. Duzick, B. Hamzavy, and J. Kelly, "Holographic optical element (hoe) imaging in dupont holographic photopolymers," in "OE/LASE'94," (International Society for Optics and Photonics, 1994), pp. 282–293.

15. F.-K. Bruder, F. Deuber, T. Facke, R. Hagen, D. Honel, D. Jurberg, M. Kogure, T. Rolle, and M.-S. Weiser, "Full-color self-processing holographic photopolymers with high sensitivity in red-the first class of instant holographic photopolymers," Journal of Photopolymer Science and Technology **22**, 257–260 (2009).

16. L. Carretero, S. Blaya, R. Mallavia, R. Madrigal, and A. Fimia, "A theoretical model for noise gratings recorded in acrylamide photopolymer materials used in real-time holography," J. Mod. Opt. **45**, 2345–2354 (1998).

17. J. V. Kelly, F. T. O'Neill, J. T. Sheridan, C. Neipp, S. Gallego, and M. Ortuno, "Holographic photopolymer materials: nonlocal polymerization-driven diffusion under nonideal kinetic conditions," J. Opt. Soc. Am. B **22**, 407–416 (2005).

18. C. Decker and A. Jenkins, "Kinetic approach of o2 inhibition in ultraviolet- and laser-induced polymerizations," Macromolecules **18**, 12411244 (1985).

19. M. Neumann, W. Miranda Jr, C. Schmitt, F. Rueggeberg and I. Correa "Molar extinction coefficients and the photon absorption efficiency of dental photoinitiators and light curing units," Journal of dentistry **33**, 525–532 (2005).

20. G. D. Love, "Wave-front correction and production of zernike modes with a liquid-crystal spatial light modulator," Appl. Opt. **36**, 1517–1520 (1997).

21. A. C. Urness, E. D. Moore, K. K. Kamysiak, M. C. Cole, and R. R. McLeod, "Liquid deposition photolithography for submicrometer resolution three-dimensional index structuring with large throughput," Light: Science & Applications **2**, e56 (2013).

1. Introduction

Gradient index (GRIN) lenses and micro-optics are important devices in photonics and opto-electronics because they offer appealing form factors, simplified mounting and packaging for many applications, and additional degrees of freedom in lens design, enabling aberration or lens element reduction. These attributes have driven applications in fiber optic communication, imaging systems, and optical medical devices.

Current methods to fabricate GRIN lenses [1] are neutron irradiation, chemical vapor deposition (CVD), ion exchange and partial polymerization. Neutron irradiation creates a GRIN distribution by changing the index of refraction of boron glass (ex. BK7 glass) by locally altering the boron concentration. The variation in the index of refraction is approximately linear to the neutron irradiation dose, enabling arbitrary and high fidelity GRIN recordings. However, large neutron doses are required to induce the index change and the fabricated GRIN pattern is not stable [2]. The CVD technique [3] fabricates GRIN lenses by sequentially depositing thin, homogeneous layers of glass materials onto a substrate. The GRIN pattern is produced by depositing glasses with different refractive indices as the volume is created, varying the refractive index distribution axially through the volume. However, CVD has limitations for large diameter lenses due to the step index formation by the deposition process and can only fabricate axial GRIN lenses. The ion exchange technique [4, 5] is the main technology used for mass production and creates GRIN lenses by diffusing ions from a bath of salt(ex. lithium bromide) into a glass substrate and replacing the ions originally residing in the glass. The ions have different densities and different refractive indices, resulting in a GRIN distribution in the glass matching the diffusion profile of the ions, with diameters ranging from 0.5 - 10 mm. However, ion diffusion profiles limit potential index profiles formed to Gaussian, Lorentzian or linear, making arbitrary GRIN distribution impossible to fabricate.

To reduce cost and increase GRIN lens performance, several methods have been developed to fabricate GRIN lenses in polymers. High resolution axial GRIN lenses can be fab-

ricated by laminating nanometer thick polymer sheets with controllable refractive index together [6]. However, this technique is limited to producing high quality axial GRIN and has not demonstrated index modulation transversely. Transverse index modulation in polymers has been demonstrated, however, these methods are either difficult to fully control, the process is time consuming or is limited in the GRIN profile they can produce. Methods include polymer GRIN lens rod fabrication through thermal treatment [7] and UV irradiation [8], large diameter, thin polymer GRIN lenses using longitudinal diffusion and multiple monomers to create the GRIN profile [9] and lithographic exposure of 100 μm - 1 mm thick polymer samples with a de-focused Gaussian beam [10]. In summary, the underlying physical principle of these methods limits their ability to fabricate high fidelity transverse GRIN lenses with arbitrary index profiles. To overcome this limitation we propose and demonstrate a new form of GRIN lens fabrication that can print complex parts with optical control over the refractive index profile.

This method utilizes optically driven diffusive photopolymers illuminated by a deformable mirror device (DMD) and a light emitting diode (LED). The absorbed light induces polymerization and monomer diffusion, resulting in a permanent volume index change determined by the total optical dose [11] without wet chemical processing. The DMD enables spatial control of the optical dose, which allows production of GRIN lenses with a complex index profile in a single step. In addition to greater control over the refractive index profile, this fabrication method and material improves upon previous work [10] by significantly reducing scatter in the sample, improving the optical clarity throughout the entire visible spectrum and improving the environmental stability by increasing the glass transition temperature of the material by 50 °C.
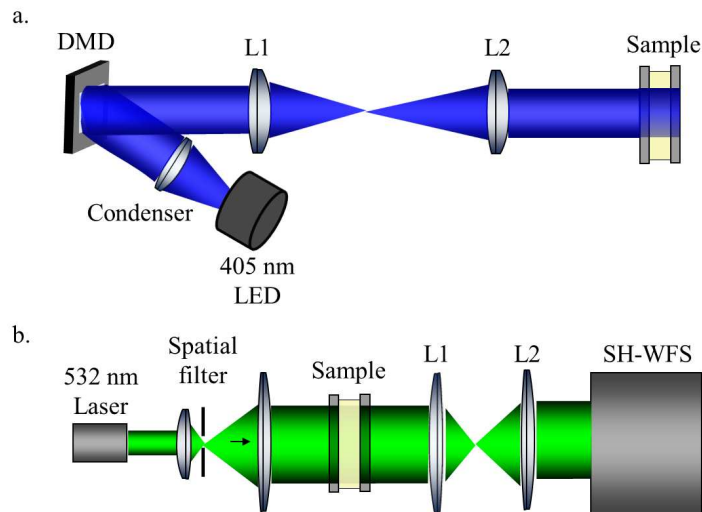

Fig. 1. Exposure and metrology system. (a) Exposure system that uses a light emitting diode (LED), Thorlabs M405L2, and deformable mirror device (DMD) to modulate the 2D intensity pattern and power of the exposure. The imaging lenses, L1 and L2, were Edmunds near-UV achromats with focal lengths of 100 mm (L1) and 75 mm (L2) and the condenser, Thorlabs ACL2520-A, had a focal length of 25mm. The DMD is a TI DLP 0.7 XGA D4100 with UV coating. (b) Metrology system that measures the refractive index profile by imaging the sample under test onto a Shack-Hartmann wavefront sensor. The lenses, L1 and L2, were Spindler and Hoyer achromats with focal lengths of 50 mm (L1) and 250 mm (L2). The Clas-2D Shack-Hartmann wavefront sensor is a Clas-XP 81000-01.

2. Exposure and metrology instrumentation

A deformable mirror device (DMD) spatial light modulator is used to modulate the 2D intensity pattern of the exposure, as shown in Fig. 1. An LED with center wavelength of 405 nm illuminates the DMD. The wavelength is chosen to lie on the upper shoulder of the photo-initiator absorption spectrum to provide high uniformity of dose in depth at sufficient photoinitiator concentration.

After exposure, the samples are kept in the dark at 60 degrees Celsius for five days, allowing polymerization and diffusion to continue. The elevated temperature accelerates the diffusion process, reducing the required development time. After the exposure and development processes have completed, a uniform optical exposure consumes the remaining photoinitiator and monomer, leaving a permanent, photoinsensitive part.

To determine the refractive index profiles of the fabricated structures, the samples are imaged onto a Shack-Hartman wavefront sensor, as shown in Fig. 1(b). The refractive index profile is quantified by relating the measured optical path difference at each location to the thickness of the sample under test.

3. Material system

Optically driven diffusive photopolymer media are an appealing material platform for GRIN lenses and micro-optics. It affords relatively high index contrasts and high sensitivity in materials that are low cost, self-processing, widely tunable and environmentally robust [12]. The media is formulated in the liquid phase so the form factor is very flexible and encapsulation of additional optical or mechanical elements is possible. The media consists of two independent chemistries, a solid, low-index matrix formed by a thermoset polymer, followed by recording into a second (typically radical) high-index photopolymer [13]. Figure 2 elucidates how the refractive index distribution is modulated in the media.
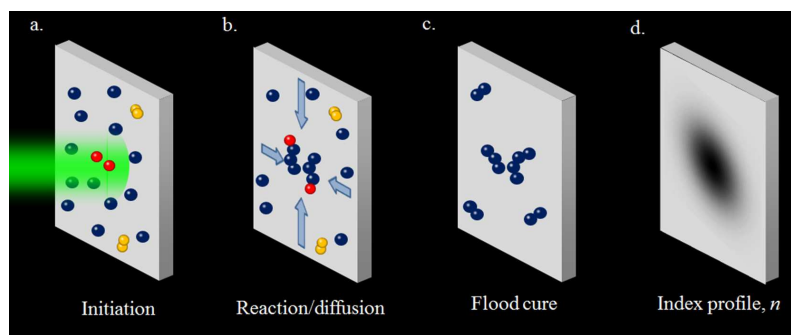

Fig. 2. Description of the index modulation mechanism in optically driven diffusive photopolymer media. The blue balls represent monomer, the yellow balls photointiator and the red balls are radicals. (a) Photons create radicals that initiate polymerization (conversion of writing monomer to polymer) at that location. (b) Replacement monomer diffuses into the reaction region (blue arrows) and the matrix swells out of it. (c) An optical flood exposure consumes all remaining chemistry leaving a higher density of high refractive index polymer and lower density of low-refractive matrix in the illuminated region. (d) Segregation of writing polymer and matrix creates the index distribution correlated to the optical dose.

Structured light creates radicals that initiate polymerization in response to the local optical dose. This creates a concentration gradient in the monomer that induces diffusion of replacement monomer into and the matrix to swell out of the reaction region, creating the index dis-

tribution through segregation of the matrix and recording polymer. Thus it is similar to ion exchange in that the refractive index profile is created through segregation and diffusion of materials with different refractive indices, however in this method the diffusion is directed by an externally applied optical pattern. Thus, the GRIN patterns are not limited to simple diffusion profiles and instead are arbitrary to within the limits of the optical pattern that can be generated and the index contrast the material can achieve.

3.1. Photopolymer formulation

The photopolymer material formulation used here, shown in Table 1, is similar to commercial two-chemistry media [14, 15] that consist of a photo-insensitive urethane matrix swollen with the mobile writing chemistry. This writing chemistry comprises a high-refractive index acrylate monomer and a small amount of photoinitiator. To formulate sample the material components, described in table 1, were mixed together, degassed and then cast between two millimeter thick glass slides at thicknesses ranging from 250 micrometers to two millimeters.

To create high quality optical components, noise gratings [16] and scatter created during the recording process must be suppressed. We hypothesize noise gratings and scatter can be reduced by separating reaction and diffusion dynamics via higher T_g media, see supplementary information. The T_g of this material is 20°C and we observe significantly less scatter than similar formulations with T_gs of -20°C or lower that is more typical of commercial holographic photopolymer media. We attribute the reduction of scatter in high T_G materials to a reduction in the photopolymerization reaction rate and extended dark polymerization that decouples feedback between optical scatter and index response.

Table 1. Material formulation. Components are used as received, except TBPA which is purified by dissolving in methylene dichloride and filtering with a Millipore 0.5 micron pore membrane filter. Components 3-6 are mixed into the polyol at 60°C, degassed, then mixed with isocyanate and cast between millimeter thick glass slides.

Component	Name	Source	wt%
Urethane Matrix			
Polyol	Polyester-block-polyether α,ω-diol	Sigma	55.61
Isocyanate	Desmodur 3900	Bayer	37.81
Plasticizer	Dibutyl phthalate	Sigma	0.5
Catalyst	Dibutyltin dilaurate	Sigma	0.01
Writing Chemistry			
Photoinitiator	(2,4,6-trimethylbenzoyl) diphenylphosphine oxide (TPO)	Sigma	0.067
Writing Monomer	(2,4,6) tribromophenyl acrylate (TBPA)	Huyang Puicheng	6.00

To increase uniformity of initiation in depth, and thus uniformity in the refractive index distribution, a small concentration of photoinitiator is used in the material. Unfortunately, this results in less sensitivity and saturating absorption across the 2D exposure profile, resulting in poor recording fidelity if not properly addressed. The saturating absorption is the result photoinitiator depletion in high intensity regions that reduces sensitivity and thus index response at large doses. This effect occurs in all systems that use an photolytic initiator but is exacerbated here because nearly all photoinitiator is consumed to maximize achievable index contrast.

3.2. Dependence of optical exposure dose on index change

Given that radical initiated photopolymers are well known [17] to have a sub-linear response to intensity and given the complex cascade of coupled processes that follow the initiation step, one would not expect this material to have a linear relation between optical dose and refractive index. However, we have shown [11] that, for weak exposures, this formulation does respond linearly to optical dose. This linearity is violated when the dose is sufficient to consume a significant fraction of the initiator, at which point the sensitivity declines, as shown in Fig. 3(a). This saturating behavior can be corrected by plotting the index response not against dose, H, but against the amount of initiator consumed, as shown in Fig. 3(b). The two are related by the exponential solution to the first-order differential equation governing the absorption and photolytic cleavage process, described below. Note that the negative intercept of the line in Fig. 3(b) is caused the threshold dose required to clear dissolved O_2 [18].
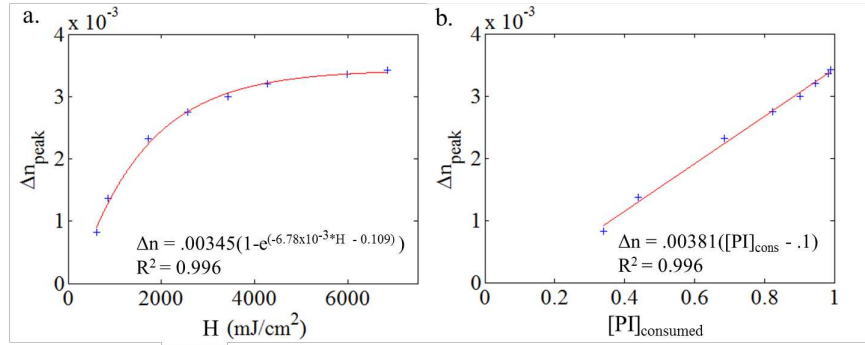

Fig. 3. Dependence of refractive index change on the optical dose, H, and the fractional photoinitiator consumption. (a) The dependence of the measured peak Δn of quadratic GRIN lenses on the exposure dose. (b) The dependence of the measured peak Δn of quadratic GRIN lenses on the fraction of photoinitiator consumed. An irradiance of 10mW/cm^2 was used for every exposure.

The rate of photoinitiator bleaching as a function of exposure dose is given by

$$[PI]_{cons} = [PI]_0(1 - \exp(-k_d I_o t)) = [PI]_0(1 - \exp(-k_d * H)) = [PI]_0(1 - \exp(\frac{-\varepsilon\phi}{N_a h\nu}H)) \quad (1)$$

where [PI] is photoinitiator concentration, I is the exposure irradiance, k_d is the bleaching rate constant, ε is the molecular absorption coefficient, ϕ is the quantum yield, N_a is Avogadro's number, h is planck's constant and ν is the center frequency of the exposure source. The assumed values of the ϕ and ε of the photoinitiator at ν are 0.8 and 240 L/(mol cm) [19], respectively, making $k_d \approx 0.015$. The equation that describes index modulation as a function of optical dose is therefore

$$\Delta n = \Delta n_{max}(1 - e^{(b*H - H_{O_2})}) \quad (2)$$

where each coefficient corresponds to a physical parameter described by equation 1. The Δn_{max} coefficient corresponds to the maximum index contrast achievable, b represents the bleaching rate constant and H_{O_2} is the oxygen clearing dose. The measured bleaching rate constant is approximately half the expected, as described by equation 1. A potential explanation for this effect is a less-than-unity efficiency of chain transfer re-initiation that results in dynamic range of the material not being used to create the patterned index distribution [11]. Although the

precise mechanism is unknown, the effect is repeatable and the dose can therefore be corrected for this effect.

In order to fabricate high fidelity structures, the dependence of the optical exposure dose on index change is used to correct the optical pattern that exposes the material. Equation 2 is inverted and applied to the desired index profile and then normalized to the bit depth of the DMD to create the exposure pattern

$$H_{corrected} = ln(1 - PI_{max} - PI_{pre})/b \qquad (3)$$

where PI_{max} is the amount of photoinitiator consumed at peak modulation and PI_{pre} is the photoinitiator consumed during the O_2 clearing precure. To verify that the amount of index modulation was not limited by a lack of photoinitiator, the photoinitiator concentration was increased by a factor of two and the experiment was repeated. While the sensitivity doubled, as expected, the maximum index modulation achieved was comparable, demonstrating maximum index modulation was not limited by photoinitiator concentration.

This behavior leads to an important material design choice. A large initiator concentration relative to that consumed will result in a nominally linear response such that the final index profile is proportional to optical dose. However, if this concentration times the molar absorptivity of the initiator causes significant absorption through the depth of the part, the index profile will not be uniform in depth. One solution to this trade-off is to chose an initiator with low absorptivity at the exposure wavelength, allowing low absorption at high concentration. Since high initiator concentration can reduce final transparency and lead to discoloring of the polymer, we demonstrate here that one can also correct the dose with the transform shown in eq. 3. This enables the use of the minimal amount of photoinitiator.

4. Experimental results

To demonstrate optical performance of components fabricated with this method, a GRIN lens with a quadratic profile with a thickness of one millimeter was fabricated and compared to a GRIN lens with an ideal phase profile. Figure 4(a) shows how the intensity correction of equation 3 results in a high fidelity recording. The fidelity was quantified by comparing the point spread function (PSF) at the focal plane, Fig. 4(c), and the lens phase profile, Fig. 4(a), to the simulated performance of a GRIN lens with an ideal phase profile, shown in Fig. 4(b) and (d). To compare how well the measured performance compared to expected performance, the root mean square (RMS) error between the measured and designed phase profile was calculated and converted to a Strehl ratio. The measured 2D phase profile had an RMS wavefront error of 0.0462 waves, corresponding to a Strehl ratio of 0.9548. The Strehl ratio of the PSF at focus was measured by a camera and was 0.942, demonstrating good agreement between measurements. Figure 4(b) shows a two-dimensional illustration of the recording error of the corrected profile. The majority of the error is located at the edge of the quadratic lens where the derivative of the index profile is greatest. This suggests the recording error could be minimized by increasing the bit depth and/or number of pixels used by the gray-scale pattern generator when exposing the structure.

To demonstrate directed GRIN function beyond the usual quadratic profile, we show in Fig. 5 the fabrication of Zernike GRIN functions. Figures 5(a) and (c) show the Zernike functions [3,3] and [-1,3] surrounded by a uniform ring representing the zero level since the Zernike polynomials have negative values and this process can only record positive phase delay. Figures 5(b) and (d) show the refractive index profile measured by the wavefront sensor. The measured Zernike patterns written in the media had a .951 and .943 correlation coefficient with their designed profiles, respectively, demonstrating high recording fidelity. To create more complex optical
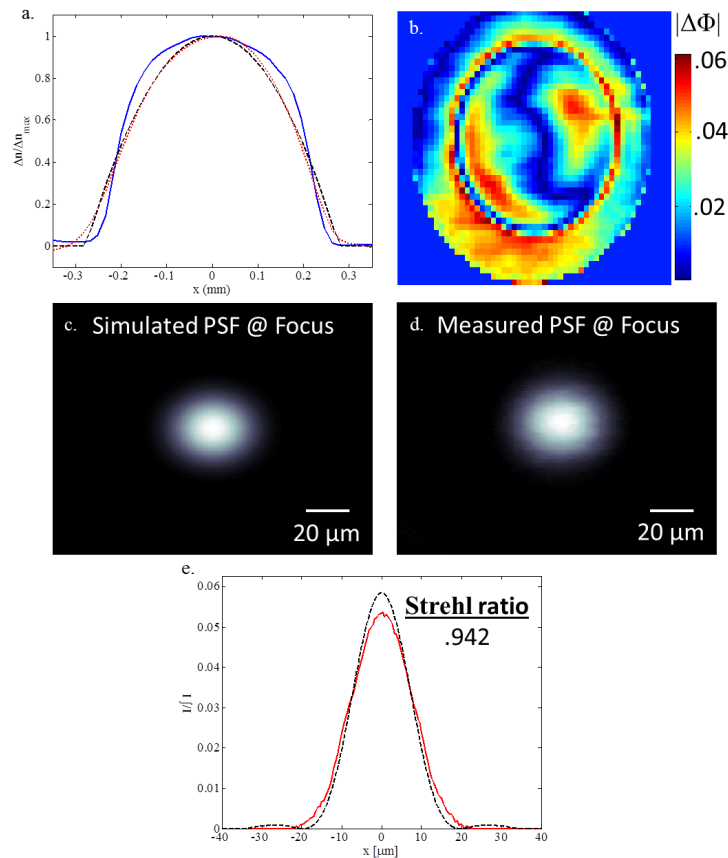
Fig. 4. Demonstration of a quadratic GRIN lens with a thickness of one millimeter fabricated in diffusive photopolymer media. (a) The index profile of the intended (black dashed), uncorrected (solid blue) and corrected (dotted red) profile. (b) Phase errors (measured in waves) of the corrected profile. (c) The simulated point spread function (PSF) at the focus of the lens. (d) The measured PSF at the focus of the lens. (e) Cross-section of the simulated (black dashed) and measured (solid red) PSF at the focus.

function or permanently remove abberations in an optical system, multiple Zernike profiles can be multiplexed together [20] in the fabricated optic.

A limit of this technique is the largest index change that the material can provide, here about $3.5 \ 10^{-3}$, although as much as 0.1 has been demonstrated [21]. The material can be made thicker to achieve higher optical path length variation, but this sacrifices transverse resolution. That is, in order to maintain a depth of focus greater than the thickness during the lithographic fabrication of the index profile, the minimum resolution scales like the square root of thickness times wavelength. However, most lens and phase profiles are slowly varying across the field, so high transverse resolution is not required and thick optics can be fabricated.

One solution to fabricating a thick, high resolution part is to stack many high resolution thin layers [21], however metrology of such structures is complex and difficult to interpret. An alternative solution is to use only one wave of optical path length and collapse the phase profile to a single layer GRIN diffractive element. Figure 6 shows phase micrographs of a flat GRIN
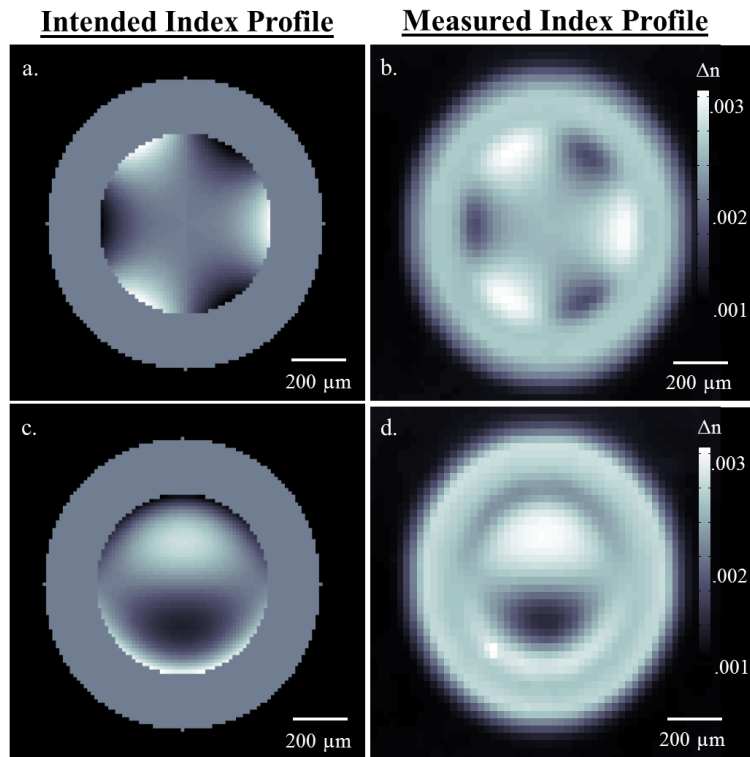
Intended Index Profile   **Measured Index Profile**

Fig. 5. Zernike phase profiles with a thickness of one millimeter fabricated in diffusive photopolymer media. (a) Intended index profile of z[3,3]. (b) Measured index profile of z[3,3]. (c) Intended index profile of z[-1,3]. (d) Measured index profile of z[-1,3]. note: The increased pixilation in (b) and (d) compared to (a) and (c) is due to the sparser sampling of the Shack-Hartmann wavefront sensor compared to the DMD pixels.
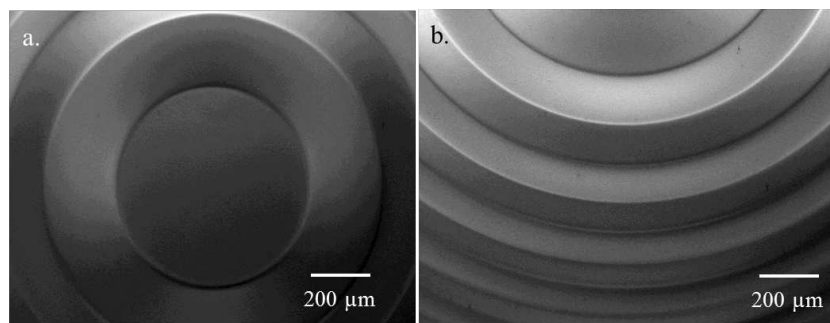

Fig. 6. Fresnel lenses with a thickness of 250 microns fabricated in diffusive photopolymer media imaged with a differential interference contrast microscope. (a) Phase micrograph of the center and the (b) edge of the Fresnel lens.

Fresnel lens. It is possible to reach a full wave of delay, even at the low index contrast used here, in less than 150 microns of thickness. This method enables a new form of refractive/diffractive

hybrid lens in which the diffractive function is within the volume, not at the lens surface.

5. Summary and conclusions

We have presented a method to fabricate arbitrary GRIN optics by patterning optically driven diffusive photopolymer media with a projection gray-scale maskless lithography instrument. The index profile is controlled by modulating the 2D intensity of the exposure pattern. We demonstrated high quality arbitrary GRIN optic fabrication by creating quadratic profile, millimeter aperture GRIN lenses, Zernike polynomials and diffractive optical elements.

The materials are formulated in the liquid phase so the form factor is very flexible, enabling the fabrication of hybrid arbitrary GRIN/refractive optical components by using a mold to form the refractive component. A further benefit is that custom arbitrary GRIN optics can be fabricated on demand, not unlike 3D printing technologies, bringing benefits of low cost small volume production, and quick turn custom and prototype components.

Acknowledgments